# Effect of material properties of the eyeball coat on optical image stability

**Wiesław Śródka**
Wroclaw University of Technology
Faculty of Deformable Body Mechanics
Wroclaw, Poland

**Barbara K. Pierscionek**
University of Ulster
School of Biomedical Sciences
Cromore Road, Coleraine, BT52 1SA,
United Kingdom

**Abstract.** The dynamics of the eyeball, most notably the changes in intraocular pressure, need to be stabilized optically to prevent noticeable changes in image quality. This control depends on the rheological properties of the eyeball coats and how the elasticity of the cornea, sclera, and limbus vary relative to one another. Nonlinear finite element modeling shows that image quality can be preserved over a range of elastic moduli. For intraocular pressure variations from 8 to 40 mm Hg, optical image stability is best for an elastic secant modulus of the cornea of 0.267 MPa. Optimal quality is achieved when the elastic moduli of the limbus and sclera are, respectively, 3.6 and 4 times that of the corneal modulus.  [DOI: 10.1117/1.2975844]

Keywords: ophthalmology; optics; elastic modulus; finite element analysis.

Paper 08080R received Mar. 5, 2008; revised manuscript received Apr. 15, 2008; accepted for publication Apr. 22, 2008; published online Sep. 10, 2008.

## 1 Introduction

The comparatively simple structure of the tissues contained in the outer eyeball is juxtaposed against an extremely precise optical system. The mechanical (elastic) properties of the outer coats of the eye are fundamentally important for maintenance of optical integrity and healthy physiological function. They are also extremely difficult to measure with accuracy. Hence, the extent of their contribution to the fine optical adjustments that the eye needs to make to maintain image quality are not known. Intraocular pressure fluctuates during the day and, without some sort of adjustment mechanism to stabilize the optics, could be expected to affect the quality of the image on the retina. Previous studies have shown no or very slight alterations in refractive power in spite of variations in the pressure of the eye[1,2] and no reported concomitant changes in image quality.[3] The maintenance of optical image quality in spite of ocular and systemic variations in fluid pressures has been hypothesized as resulting from the stabilizing influence of the limbus.[4] Kasprzak[5] has further suggested that displacements of the corneal apex with intraocular pressure changes may be compensated by a change in corneal radius that has the opposite effect on focussing to that of the apical displacement. Whether or not this hypothesis has support depends on the elastic properties of the cornea and sclera and how these compare with the elasticity of the limbus.

The elastic properties of the cornea and sclera, as well as the influence of the limbus on maintenance of image quality, have been tested in previous studies using linear models (i.e., single values of elasticity moduli for each tissue)[6,7]. This study extends the investigations to a nonlinear model, which would be closer to the tissue properties and, hence, would be more accurate over larger ranges of intraocular pressure change, and investigates the optimal mechanical properties of the cornea, sclera, and limbus that would be required for maintaining stability of the optical image.

The models are tested for a range of different corneal, scleral, and limbal material properties. Three materials are selected for the cornea and these reflect findings reported in the literature for material constants[8,9] and elasticity moduli.[10] Scleral and limbal material properties are chosen to optimize image quality.

## 2 Methods

### 2.1 *Finite Element Modeling*

The modeling of the eye follows a method used in an earlier paper.[11] Briefly, COSMOS/M standard software (Structural Research and Analysis Corporation, Santa Monica, California) was used to construct an eye model that is a two-dimensional, quadrilateral 8-node body of elements of revolution; the model consisted of over 500 elements. The model was used to investigate changes in material properties and response to loading. Further calculations, involving the optical analysis of the eye and changes with intraocular pressure, were performed using software developed by the one of the authors (W. Srodka).

### 2.2 *Numerical Model of the Eye*

The eye model was assumed to be axially symmetric. The external surface of the sclera was approximated with a sphere of 12.5-mm radius, a thickness of 1 mm at the optic nerve, 0.6 mm in the equatorial zone, and 0.8 mm at the limbus (Fig. 1).

External and internal cornea profiles were described by the following ellipse:

Address all correspondence to B. K. Pierscionek, School of Biomedical Sciences, University of Ulster, Cromore Rd., Coleraine, BT52 1SA, United Kingdom. E-mail: b.pierscionek@ulster.ac.uk

1083-3668/2008/13(5)/054013/6/$25.00 © 2008 SPIE

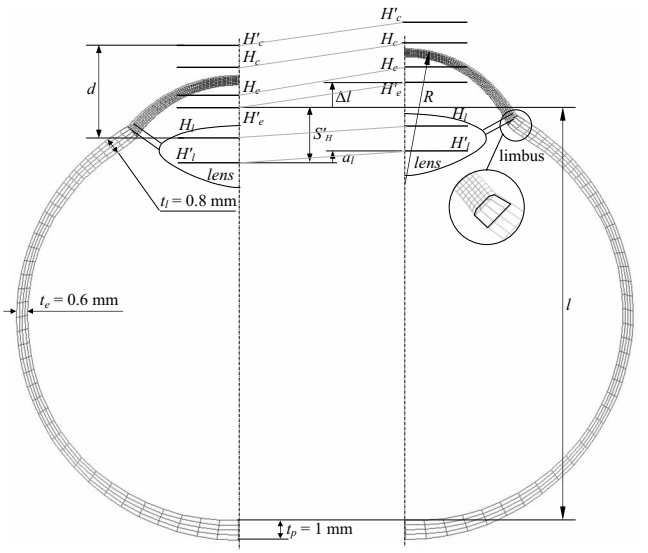


**Fig. 1** Diagrammatic representation of the eyeball model showing location of the main optical planes and the changes in corneal geometry and position with loading [change in intraocular pressure ($p$)].

$$z(x) = \frac{1}{e^2 - 1} \cdot [\sqrt{R^2 + x^2(e^2 - 1)} - R]$$

where $R$ is the corneal radius of curvature at the apex and $e$ is eccentricity, which in all models=0.5.

Table 1 shows the basic geometrical and optical parameters of the model when free from any load. Most parameters are compatible with the human eyeball model of Gullstrand-Le Grand[12] with additional parameters from experimental studies.[13–16]

## 2.3 *Optical System of the Eye*

The optical system of the model eye consists of a deformable cornea and a lens with constant refracting power (the model assumes a constant accommodative state). There is no independent movement of the lens. As the intraocular pressure ($p$) increases, the optically self-adjusting eye maintains a focussed image on the retina and the lens is displaced by a distance equal to the limbal displacements. In all results, $p$ is given as a dimensionless multiplier of the nominal intraocular pressure: $p=1$, which represents 2.135 kPa (16 mm Hg). The optical system and the finite element model of the eye, in its initial state and after loading, are shown in Fig. 1.

The total refracting power of the eye ($P_{\text{eye}}$) is the sum of the refractive powers of the cornea ($P_{\text{cornea}}$) and the lens ($P_{\text{lens}}$)

$$P_{\text{eye}} = P_{\text{cornea}} + P_{\text{lens}} - \frac{dP_{\text{cornea}}P_{\text{lens}}}{n}. \quad (1)$$

The refractive index of the cornea is taken as 1.377,[15] and that of the aqueous and vitreous humors as 1.336.[12] The distance $d$ between the back principal plane of the cornea ($H'_c$) and the front principal plane of the lens ($H_l$) changes during loading and influences the power of the eye ($P_{\text{eye}}$) (Fig. 1).

**Table 1** Biometric and material parameters used in the finite element model.

| Parameter | Value |
|---|---|
| Axial radius of anterior corneal curvature[a] | $R$=7.80 mm |
| Axial radius of posterior corneal curvature[a] | $r$=6.49 mm |
| Central corneal thickness[b,c] | $CCT$=0.520 mm |
| Peripheral corneal thickness adjacent to limbus[a] | $PCT$=0.750 mm |
| Diameter of the cornea[d] | 11.5 mm |
| Refractive index of aqueous and vitreous humours[a] | $n$=1.336 |
| Refractive index of the cornea[e] | $n$=1.377 |
| Refractive power of lens[a] | $P_{\text{lens}}$=22.07 D |
| Poissons ratio[f] | $\nu$=0.49 |
| Nominal intraocular pressure[c] | $IOP$=2.135 kPa (16 mm Hg) |

[a]Reference 9.
[b]Reference 10.
[c]Reference 13.
[d]Reference 11.
[e]Reference 12.
[f]Reference 15.

The refractive power of the cornea depends on the axial radius of curvature $R$, on its external profile and on its refractive index ($n$)

$$P_{\text{cornea}} = \frac{n-1}{R}. \quad (2)$$

Initially, at $p=0$, the length $l$ [the distance from the back principal plane of the eye ($H'_e$) to the retina] is equal to the focal length $f$ of the eye

$$f = \frac{n}{P_{\text{eye}}}. \quad (3)$$

When a load is applied ($p>0$), the eyeball expands and the limbus and lens are displaced anteriorly by $a_l$, causing an increase in $l$ by

$$\Delta l = a_l + \Delta S'_H. \quad (4)$$

Where $\Delta S'_H$ is an increment of distance between $H'_l$ and $H'_e$

$$S'_H = d\frac{P_{\text{cornea}}}{P_{\text{eye}}}.$$

As a result, the focus of the optical system shifts by distance $B$

$$B = \Delta l - \Delta f. \quad (5)$$

**Table 2** Material parameters tested

| Material | $A$ [Pa] | $\alpha$ | $E_o$ [MPa] | $E_{secant}$ [MPa] |
|---|---|---|---|---|
| M1 | 100 | 83.0 | 0.0083 | 0.313 |
| M2 | 200 | 61.6 | 0.0123 | 0.267 |
| M3 | 800 | 39.0 | 0.0312 | 0.239 |

The function $B(p)$ is the change in distance of the image from the fundus with change in $p$. The analytical condition for optical self-adjustment is expressed as follows:

$$\frac{dB}{dp} = 0. \tag{6}$$

## 2.4 *Material Properties*

### 2.4.1 *Cornea*

The cornea is modeled as a two-dimensional, isotropic structure with nonlinear material properties. Errors resulting from assuming isotropy in previous models have been found to be negligible.[17] Several suggestions for nonlinear characteristics of eye tissue material are found in the literature. The best one, empirically justified, yet simple and easy to use, is the exponential function recommended by Fung[18]

$$\sigma = A[\exp(\alpha\varepsilon) - 1] \quad \text{for a strain } \varepsilon \geqslant 0, \tag{7}$$

where $\sigma$ is the stress, $\varepsilon$ is the strain, and $A$ and $\alpha$ are material constants. The tangential elasticity modulus $E_{\text{tangent}} = d\sigma/d\varepsilon$, which represents the instantaneous rate of change of stress as a function of strain, is expressed by

$$E_{\text{tangent}} = A\alpha\exp(\alpha\varepsilon) = \alpha(\sigma + A),$$

which, when $\sigma \to 0$, becomes

$$E_o = A\alpha. \tag{8}$$

For negative strain/stress values (compression test), the linear constitutive equation is assumed:

$$\sigma = E_o\varepsilon, \quad \varepsilon < 0. \tag{9}$$

For a given stress, the major tensors are reduced to stress along a single axis[19] by the formula

$$\sigma^* = \{(1/2)[(\sigma_1 - \sigma_2)^2 + (\sigma_1 - \sigma_3)^2 + (\sigma_2 - \sigma_3)^2]\}^{0.5}.$$

The major strain tensors can be reduced in a similar way

$$\varepsilon^* = \{(2/9)[(\varepsilon_1 - \varepsilon_2)^2 + (\varepsilon_1 - \varepsilon_3)^2 + (\varepsilon_2 - \varepsilon_3)^2]\}^{0.5}.$$

Three selected materials, used for testing the model, are shown in Table 2. The studies of Friedenwald[20] on corneal rigidity and investigations of corneal apical displacement with changes in intraocular pressure[21] suggest that M2 (Table 2), may be the optimal material for the human cornea.

### 2.4.2 *Sclera*

The (secant) elasticity modulus $E_{\text{sec}}$, for any nonlinear material, can only be made for arbitrarily defined conditions (at the same point, for the same external load, with identical deformations). In the case of two materials (cornea and sclera) in this model, it is possible to find the scleral modulus that satisfies the equation

$$\frac{E_{\text{sec sclera}}}{E_{\text{sec cornea}}} = Q_{\text{sclera}}, \tag{10}$$

independently of $p$ (i.e., for any applied stresses). However, it is necessary to introduce an additional condition: $\sigma = const_1$, or $\varepsilon = \text{const}_2$; it is assumed that Eq. (10) is satisfied for a fixed stress (i.e., $\sigma = \text{const}_1$), which arises from the assumed geometrical stability of the model.

The secant modulus $E_{\text{sec}}$, for a selected point in the stress-strain curve $\sigma(\varepsilon)$, is a slope of the line passing through that point and the origin of the co-ordinate system

$$E_{\text{sec}} = \frac{\sigma}{\varepsilon}.$$

Because

$$E_{\text{sec sclera}} = \frac{\sigma}{\varepsilon_{\text{sclera}}}, \quad \text{and } E_{\text{sec cornea}} = \frac{\sigma}{\varepsilon_{\text{cornea}}}.$$

then

$$\frac{E_{\text{sec sclera}}}{E_{\text{sec cornea}}} = \frac{\sigma/\varepsilon_{\text{sclera}}}{\sigma/\varepsilon_{\text{cornea}}} = \frac{\varepsilon_{\text{cornea}}}{\varepsilon_{\text{sclera}}} = Q_{\text{sclera}}. \tag{11}$$

At the limit, when $\varepsilon \to 0$, $E_{sec} \to E_{tangent}$ and from Eq. (8)

$$\frac{E_{\text{sec sclera } o}}{E_{\text{sec cornea } o}} = \frac{A_{\text{sclera}}\alpha_{\text{sclera}}}{A_{\text{cornea}}\alpha_{\text{cornea}}} = Q_{\text{sclera}}. \tag{12}$$

Comparing the stress in both materials

$$\sigma = A_{\text{sclera}}[\exp(\alpha_{\text{sclera}}\varepsilon) - 1] = A_{\text{cornea}}[\exp(\alpha_{\text{cornea}}\varepsilon) - 1]. \tag{13}$$

From Eq. (12), Eq. (11) will be satisfied when

$$\frac{\alpha_{\text{sclera}}}{\alpha_{\text{cornea}}} = Q_{\text{sclera}} \tag{14a}$$

and

$$A_{\text{sclera}} = A_{\text{cornea}}. \tag{14b}$$

### 2.4.3 *Limbus*

Although the material properties of the limbus are anisotropic,[22] the limbal area is very small (relative to the corneal and scleral areas) and so the limbal material properties are taken as isotropic in the model. As in case of sclera, the elastic properties of the limbus are adjusted relative to those of the cornea

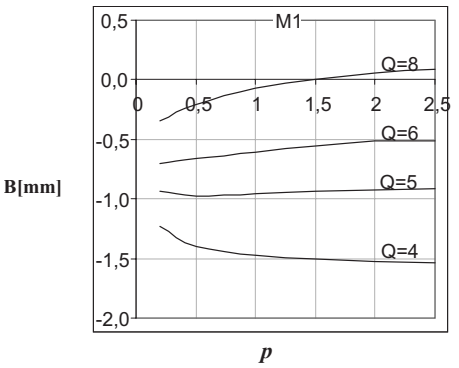


**Fig. 2** Shift in optical focus B plotted against intraocular pressure $p$ for an eye model with a cornea of material M1 (described in Table 2) for varying values of $Q_{\text{sclera}}$.

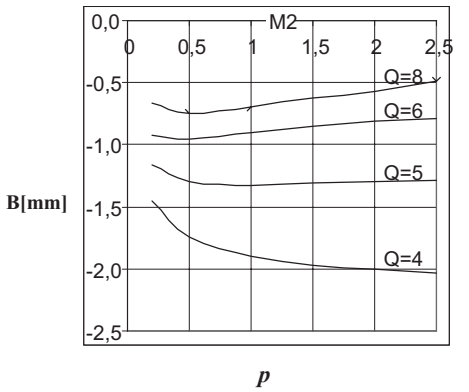


**Fig. 3** Shift in optical focus B plotted against intraocular pressure $p$ for an eye model with a cornea of material M2 (described in Table 2) for varying values of $Q_{\text{sclera}}$.

$$\frac{\alpha_{limbus}}{\alpha_{cornea}} = Q_{limbus}, \tag{15a}$$

$$A_{limbus} = A_{cornea} = A. \tag{15b}$$

#### 2.4.4 *Poisson's ration* ($\nu$)

For incompressible media, Poisson's ratio=0.5. A smaller value of $\nu$=0.49, which is commonly accepted in biological materials[18] is used in the model.

### 2.5 *Mechanical Conditions for Optical Self-Adjustment*

For each material property (M1, M2, M3) tested, conditions (10) and (13) were satisfied. As the modeling sought to optimize the material parameters of the limbus to test for the condition at which optical adjustment to mechanical forces can be made, the limbal material property values were varied, within the restrictions imposed by Eq. (14a) and (14b). Different material properties of the sclera and limbus were tested to determine those for which the model becomes optically self-adjusting, in accordance with the conditions given in Eqs. (5) and (6).

Optimization of material properties involved two stages. Firstly, finding the optimal value of $Q_{\text{sclera}}$ for which the variability in the image position with changing $p$ is minimized, that is, the values for which the image position is most stable in response to intraocular pressure increase. Secondly, using these optimal values of $Q_{\text{sclera}}$, the quotient $Q_{\text{limbus}}$, was varied to find the material parameters needed for optical self-adjusment to occur, that is, where the image position is most stable with changing $p$.

## 3 Results

Figure 2 shows the variation of image position $B$ as a function of variation in $p$ for various values of $Q_{\text{sclera}}$, from 4 to 8 and with M1 parameters for the cornea. When the scleral modulus is four times that of the corneal ($Q_{\text{sclera}}$=4), there is a movement of the optical focus in the posterior direction. For higher values of $Q_{\text{sclera}}$, the reverse occurs: the optical focus shifts anteriorly with increasing $p$. Results for a model using M2 material parameters for the cornea are presented in Fig. 3. Compared with M1 (Fig. 2), there is less variability of image position with changing $p$ for all values of $Q_{\text{sclera}}$. The most stable image position occurs when $Q_{\text{sclera}}$=5 with almost no change in focal point from $p$=0.5 to $p$=2.5. For the model using M3 material parameters (Fig. 4), there is greater variability of image position with $p$ than for either of the other models. The most stable image position is found for $Q_{\text{sclera}}$=6; stability occurs between $p$=1 and $p$=2.5.

As least variability in optical focus, with change in $p$, was found using M2 parameters for the cornea, this was used to find the optimum value for $Q_{\text{limbus}}$. Figure 5 shows the change in image position, with changing $p$, for a series of different values of $\alpha_{\text{limbus}}$, using M2 parameters for the cornea and with $Q_{\text{sclera}}$=5. As $Q_{\text{limbus}}$ increases from 1 to 5 ($\alpha_{\text{limbus}}$ increases from 61.6 to 308), the material properties of the limbus range from being identical to the cornea ($Q_{limbus}$=1) to being identical to the sclera ($Q_{\text{limbus}}$=5). For values of $Q_{\text{limbus}}$=1, 2, and 3, the image position is relatively stable between $p$=0.5 and $p$=2.5. With higher values, representing increasing limbal rigidity, there is a greater variability in image position with changing $p$. A second model tested using M2 material for the cornea and $Q_{\text{sclera}}$=4 (Fig. 6) shows that even greater stability of image position with $p$ can be achieved: The most stable image position with changing $p$, out of all models tested, was

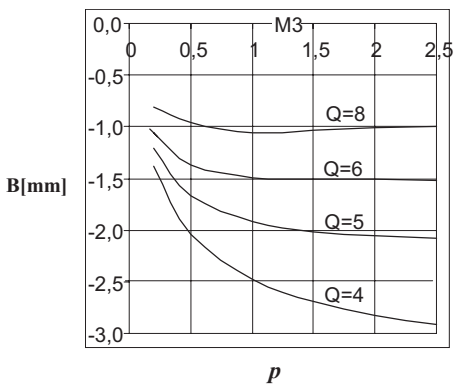


**Fig. 4** Shift in optical focus B plotted against intraocular pressure $p$ for an eye model with a cornea of material M3 (described in Table 2) for varying values of $Q_{\text{sclera}}$.

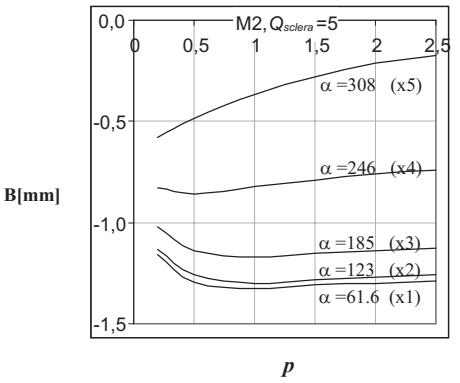


**Fig. 5** Shift in optical focus B plotted against intraocular pressure $p$ for an eye model with a cornea of material M2 (described in Table 2), $Q_{sclera}=5$ for varying values of limbal rigidity $\alpha$ (multipliers in parentheses indicate the ratio $Q_{limbus}$).

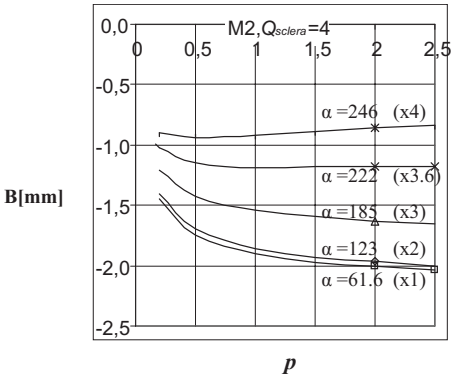


**Fig. 6** Shift in optical focus B plotted against intraocular pressure $p$ for an eye model with a cornea of material M2 (described in Table 2), $Q_{sclera}=4$ for varying values of limbal rigidity $\alpha$ (multipliers in parentheses indicate the ratio $Q_{limbus}$).

found to occur when $Q_{limbus}=3.6$ and $Q_{sclera}=4$. The values of apical corneal radius of curvature ($R$) and the shift in optical focus ($B$) for varying values of $p$ are shown in Table 3 for this optimal model.

## 4 Discussion

The outer coats of the eyeball: the sclera and cornea, need to be sufficiently firm to maintain stability in the optics of the eye and yet require some malleability to allow for fine adjustments when the pressure within the eye alters. This occurs physiologically: diurnal variations in intraocular pressure are well documented. It can also occur pathologically as seen in glaucoma when the intraocular pressure rises to levels that can eventually lead to vision loss. It has been theorized that the optical adjustability of the eye is the result of a stabilizing force induced by the limbal ring and that this acts to maintain the shape and hence refractive power of the cornea and that of the eye.[4] The limbal ring has a particular collagen arrangement[23,24] that suggests it has different material properties to those of the cornea and sclera. However, these anatomical findings do not necessarily indicate that the limbus is exclusively responsible for stabilizing the optics of the eye. If the eyeball is to maintain its refractive power with changes in intraocular pressure, the material properties of all parts of the outer eye need to be balanced relative to one another to make the fine adjustments that may be necessary.

**Table 3** Apical radius of curvature and shift of optical focus with varying intraocular pressure for eye model with material M2 for the cornea, $Q_{limbus}=3.6$ and $Q_{sclera}=4$

| Intraocular pressure [mm Hg] (as dimensionless variable) $p$ | Apical radius of curvature $R$ [mm] | Shift of optical focus $B$ [mm] |
|---|---|---|
| 8 (0.5) | 8.4269 | −1.1452 |
| 16 (1.0) | 8.4673 | −1.1862 |
| 24 (1.5) | 8.4762 | −1.1776 |
| 32 (2.0) | 8.4840 | −1.1745 |
| 40 (2.5) | 8.4894 | −1.1728 |

The results of this work show that the optical quality of the eye, as determined by the position of focus of the image, can be relatively stable over a range of intraocular pressure values from 8 to 40 mm Hg. In the first stage of the optimization process, the greatest degree of stability was obtained for a cornea of $E_{secant}=0.267$ MPa and a scleral elasticity modulus 5 times that of the cornea. A ratio of 5:1 for scleral modulus to corneal modulus supports previous studies.[7,25] For such a model, the shift of image position is 35 $\mu$m over a range of intraocular pressure from 8 to 40 mm Hg. This equates to a change of 0.1 D in refractive power, which is too low to be detected by the eye. Further optimization, to include the limbal material properties, shows an even more stable image position with intraocular pressure when the scleral modulus is 4 times that of the cornea and the limbal modulus is 3.6 times its corneal counterpart. In such a model, the limbus is slightly less rigid than the sclera and the role of limbal ring in optical self-adjustment is, therefore, slightly less significant. This supports the findings of Hjortdal,[22] who suggested that any adjustment of the optical image may be predominantly influenced by the sclera.

In previous studies using linear models,[6,7] the function of image position with changing intraocular pressure $[B(p)]$ showed much narrower ranges of $p$ for which any optical adjustment could be made. The nonlinear models presented in this study show greater stability of image position with changing pressure. Hence, even though an optimum model for image stability was found, there may be a range of corneal, scleral, and limbal elastic moduli that may adequately adjust the optics of the eye to compensate for variations in intraocular pressure. A greater range of possible moduli required for image stability is advantageous for the physiology of the eye as it would take into account the fact that elasticity of the outer coats of the eye may have individual variations and will alter with age.

## 5 Conclusions

Nonlinear finite element modeling of the eyeball shows that stability of the optical image can be sustained over a wider

range of intraocular pressures than had been suggested by previous linear models. There is no indication that maintenance of image stability depends exclusively on the properties of the limbus but rather that elastic moduli from all sections of the eyeball coat: the cornea, sclera, and limbus, and their relationships to each other all play a role.

## References


1. C. W. McMonnies and G. C. Boneham, "Experimentally increased intraocular pressure using digital forces," *Eye Contact Lens* **33**, 124–129 (2007).
2. M. Asejczyk-Widlicka and B. K. Pierscionek, "Fluctuations in intraocular pressure and the potential effect on aberrations of the eye," *Br. J. Ophthamol.* **91**, 1054–1058 (2007).
3. H. Davson, "The aqueous humour and the intraocular pressure," in *Physiology of the Eye*, H. Davson, Ed., 3–65, Macmillan Academic and Professional Ltd., London (1990).
4. D. M. Maurice, "Mechanics of the cornea," in *The Cornea*, H. D. Cavanagh, Ed., pp 187–193, Raven Press, New York (1988).
5. H. Kasprzak, "A model of inhomogeneous expansion of the cornea and stability of its focus," *Ophthalmic Physiol. Opt.* **17**, 133–136 (1997).
6. M. Asejczyk-Widlicka, D. W. Śródka, H. Kasprzak, H. , and D. R. Iskander, "Influence of intraocular pressure on geometrical properties of a linear model of the eyeball: Effect of optical self-adjustment," *Optik (Jena)* **115**, 517–524 (2004).
7. M. Asejczyk-Widlicka, D. W. Śródka, H. Kasprzak, and B. K. Pierscionek, "Modeling the elastic properties of the anterior eye and their contribution to maintenance of image quality: the role of the limbus," *Eye* **21**, 1087–1094 (2007).
8. L. S. Nash, P. R. Greene, and C. S. Foster, "Comparison of mechanical properties of keratoconus and normal corneas," *Exp. Eye Res.* **35**, 413–423 (1982).
9. C. R. Ethier, M. Johnson, and J. Ruberti, "Ocular biomechanics and biotransport," *Annu. Rev. Biomed. Eng.* **6**, 249–273 (2004).
10. E. Sjontoft and C. Edmund, "In vivo determination of Young's modulus for the human cornea," *Bull. Math. Biol.* **49**, 217–222 (1987).
11. W. Srodka and R. Iskander, "An optically inspired biomechanical model of the human eyeball," *J. Biomed. Opt.* **13**, 044034 (2008).
12. Y. Le Grand, and S. G. El Hage, *Physiological Optics*, Springer Series in Optical Sciences, Vol. **13**, Springer-Verlag, Berlin (1980).
13. Z. Liu, A. J. Huang, and S. C. Pflugfelder, "Evaluation of corneal thickness and topography in normal eyes using the Orbscan corneal topography system," *Br. J. Ophthamol.* **83**, 774–778 (1999).
14. M. Baumeister, E. Terzi, Y. Ekici, and T. Kohnen, "Comparison of manual and automated methods to determine horizontal corneal diameter," *J. Cataract Refractive Surg.* **30**, 374–380 (2004).
15. S. Patel, J. Marshall, and F. W. Fitzke, 3rd, "Refractive index of the human corneal epithelium and stroma," *J. Refract. Surg.* **11**, 100–105 (1995).
16. T. Eysteinsson, F. Jonasson, H. Sasaki, A. Arnarsson, T. Sverrisson, K. Sasaki, E. Stefánsson, and the Reykjavik Eye Study Group, "Central corneal thickness, radius of the corneal curvature and intraocular pressure in normal subjects using noncontact techniques: Reykjavik Eye Study," *Acta Ophthalmol. Scand.* **80**, 11–15 (2002).
17. H.-L. Yeh, T. Huang, and R. A. Schachar, "A closed shell structured eyeball model with application to radial keratotomy," *J. Biomech. Eng.* **122**, 504–510 (2000).
18. Y. C. Fung, *Biomechanics: Mechanical Properties of Living Tissues*. Springer-Verlag, N.Y. (1993).
19. R. Hill, *Plasticity*, Oxford University Press, London (1950).
20. J. S. Friedenwald, "Contribution to the theory and practice of tonometry," *Am. J. Ophthalmol.* **20**, 985–1024 (1937).
21. M. R. Bryant and P. J. McDonnell, "Constitutive laws for biomechanical modeling of refractive surgery," *J. Biomech. Eng.* **118**, 473–481 (1996).
22. J. Ø. Hjortdal, "Regional elastic performance of the human corne," *J. Biomech.* **29**, 931–942 (1996).
23. R. H. Newton and K. M. Meek, "Circumcorneal annulus of collagen fibrils in the human limbus," *Invest. Ophthalmol. Visual Sci.* **39**, 1125–1134 (1998).
24. H. Aghamohammadzadeh, R. Newton, and K. Meek, "X-ray scattering used to map the preferred collagen orientation in the human cornea and limbus," *Structure (London)* **12**, 249–256 (2004).
25. S. L.-Y. Woo, A. S. Kobayashi, W. A. Schlegel, and C. Lawrence, "Nonlinear material properties of intact cornea and sclera," *Exp. Eye Res.* **14**, 29–39 (1972).